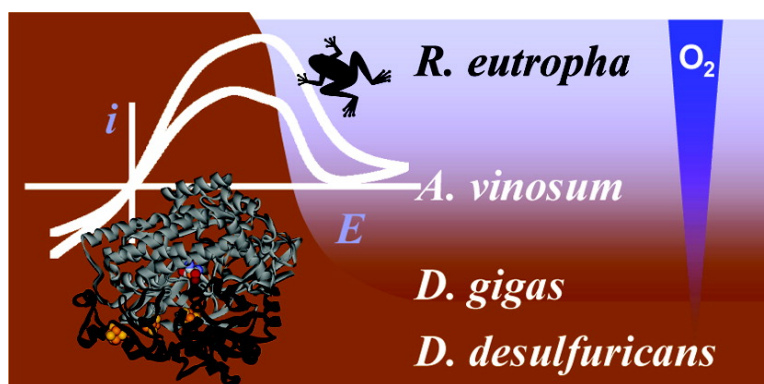


## Electrochemical Definitions of O<sub>2</sub> Sensitivity and Oxidative Inactivation in Hydrogenases

Kylie A. Vincent, Alison Parkin, Oliver Lenz, Simon P. J. Albracht, Juan C. Fontecilla-Camps, Richard Cammack, Brbel Friedrich, and Fraser A. Armstrong

*J. Am. Chem. Soc.*, **2005**, 127 (51), 18179-18189 • DOI: 10.1021/ja055160v • Publication Date (Web): 01 December 2005

Downloaded from <http://pubs.acs.org> on March 25, 2009



### More About This Article

Additional resources and features associated with this article are available within the HTML version:

- Supporting Information
- Links to the 21 articles that cite this article, as of the time of this article download
- Access to high resolution figures
- Links to articles and content related to this article
- Copyright permission to reproduce figures and/or text from this article

[View the Full Text HTML](#)

## Electrochemical Definitions of O<sub>2</sub> Sensitivity and Oxidative Inactivation in Hydrogenases

Kylie A. Vincent,<sup>†</sup> Alison Parkin,<sup>†</sup> Oliver Lenz,<sup>‡</sup> Simon P. J. Albracht,<sup>§</sup>  
Juan C. Fontecilla-Camps,<sup>¶</sup> Richard Cammack,<sup>#</sup> Bärbel Friedrich,<sup>‡</sup> and  
Fraser A. Armstrong<sup>\*†</sup>

Contribution from the Inorganic Chemistry Laboratory, University of Oxford, South Parks Road, Oxford OX1 3QR, U.K., Institut für Biologie/Mikrobiologie, Humboldt-Universität zu Berlin, Chausseestrasse 117, 10115 Berlin, Germany, Swammerdam Institute for Life Sciences, University of Amsterdam, Nieuwe Achtergracht 166, NL-1018 WV Amsterdam, The Netherlands, Laboratoire de Cristallographie et de Cristallogenèse des Protéines, Institut de Biologie Structurale J.P. Ebel (CEA-CNRS-UJF), 41 rue Jules Horowitz, 38027 Grenoble Cédex 1, France, and King's College London, Pharmaceutical Sciences Research Division, Franklin-Wilkins Building, 150 Stamford Street, London SE1 9NH, U.K.

Received July 29, 2005; E-mail: fraser.armstrong@chem.ox.ac.uk

**Abstract:** A new strategy is described for comparing, quantitatively, the ability of hydrogenases to tolerate exposure to O<sub>2</sub> and anoxic oxidizing conditions. Using protein film voltammetry, the inherent sensitivities to these challenges (thermodynamic potentials and rates of reactions) have been measured for enzymes from a range of mesophilic microorganisms. In the absence of O<sub>2</sub>, all the hydrogenases undergo reversible inactivation at various potentials above that of the H<sup>+</sup>/H<sub>2</sub> redox couple, and H<sub>2</sub> oxidation activities are thus limited to characteristic "potential windows". Reactions with O<sub>2</sub> vary greatly; the [FeFe]-hydrogenase from *Desulfovibrio desulfuricans* ATCC 7757, an anaerobe, is irreversibly damaged by O<sub>2</sub>, surviving only if exposed to O<sub>2</sub> in the anaerobically oxidized state (which therefore affords protection). In contrast, the membrane-bound [NiFe]-hydrogenase from the aerobe, *Ralstonia eutropha*, reacts reversibly with O<sub>2</sub> even during turnover and continues to catalyze H<sub>2</sub> oxidation in the presence of O<sub>2</sub>.

### Introduction

Hydrogenases are metalloenzymes that catalyze one of the simplest chemical reactions—the interconversion between H<sub>2</sub> and protons (H<sup>+</sup><sub>aq</sub>); so, not surprisingly, understanding, exploiting, and mimicking the catalytic properties of hydrogenases poses exciting scientific challenges that are highly relevant to the future of H<sub>2</sub> as an energy carrier.<sup>1–4</sup> The active sites consist of 1st-row transition metals (Fe or Fe and Ni) coordinated by

thiolates and diatomic ligands (CN<sup>-</sup> and CO)<sup>5,6</sup> and may be at least as competent as Pt-based catalysts.<sup>7</sup> However, although hydrogenases are highly active enzymes, they are generally considered to be inactivated under oxidizing conditions.<sup>1</sup> This term refers to both direct reaction with O<sub>2</sub> and reactions with anoxic oxidizing agents (including other electron acceptors in the cell), noting also that inactivation by these "side reactions" can be permanent or temporary. Hydrogenases are widespread throughout the microbial world; therefore, resolving this oxidative sensitivity is important for understanding how microorganisms have evolved to survive in aerobic environments<sup>8</sup> and vital if these enzymes (or synthetic catalysts based on their active sites)<sup>3</sup> are to be used in hydrogen cycling technologies.<sup>2,4</sup> For example, there is much interest in replacing Pt as a catalyst in fuel cells<sup>4</sup> and in developing new electrolytic and photolytic catalysts for H<sub>2</sub> production.<sup>2</sup> Consequently, a major question is how to measure and compare oxidative inactivation and reactivation among different hydrogenases and to establish quantitative parameters for defining, at the chemical level, "tolerance to O<sub>2</sub>".

<sup>†</sup> University of Oxford.

<sup>‡</sup> Humboldt-Universität zu Berlin.

<sup>§</sup> University of Amsterdam.

<sup>¶</sup> Institut de Biologie Structurale J.P. Ebel.

<sup>#</sup> King's College London.

- (1) Cammack, R.; Frey, M.; Robson, R. *Hydrogen As a Fuel: Learning From Nature*; Taylor and Francis: London and New York, 2001.
- (2) Cohen, J.; Kim, K.; Posewitz, M.; Ghirardi, M. L.; Schulten, K.; Seibert, M.; King, P. *Biochem. Soc. Trans.* **2005**, *33*, 80–82. Ghirardi, M. L.; King, P. W.; Posewitz, M. C.; Maness, P. C.; Fedorov, A.; Kim, K.; Cohen, J.; Schulten, K.; Seibert, M. *Biochem. Soc. Trans.* **2005**, *33*, 70–72. Ghirardi, M. L.; Zhang, L.; Lee, J. W.; Flynn, T.; Seibert, M.; Greenbaum, E.; Melis, A. *Tibtech* **2000**, *18*, 506–511.
- (3) Boyke, C. A.; van der Vlugt, J. I.; Rauchfuss, T. B.; Wilson, S. R.; Zampella, G.; De Gioia, L. *J. Am. Chem. Soc.* **2005**, *127*, 11010–11018. Tard, C.; Liu, X.; Ibrahim, S. K.; Bruschi, M.; De Gioia, L.; Davies, S. C.; Yang, X.; Wang, L.-S.; Sawers, G.; Pickett, C. J. *Nature* **2005**, *433*, 610–613. Zhao, X.; Chiang, C.-Y.; Miller, M. L.; Rampersad, M. V.; Darensburg, M. Y. *J. Am. Chem. Soc.* **2003**, *125*, 518–524.
- (4) (a) Karyakin, A. A.; Morozov, S. V.; Karyakina, E. E.; Zorin, N. A.; Pereygin, V. V.; Cosnier, S. *Biochem. Soc. Trans.* **2005**, *33*, 73–75. (b) Tye, J. W.; Hall, M. B.; Darensburg, M. Y. *Proc. Natl. Acad. Sci. USA* **2005**, *102*, 16911–16912. (c) Vincent, K. A.; Cracknell, J. A.; Lenz, O.; Zebger, I.; Friedrich, B.; Armstrong, F. A. *Proc. Natl. Acad. Sci. USA* **2005**, *102*, 16951–16954.

(5) Volbeda, A.; Garcia, E.; Piras, C.; De Lacey, A. L.; Fernandez, V. M.; Hatchikian, E. C.; Frey, M.; Fontecilla-Camps, J. C. *J. Am. Chem. Soc.* **1996**, *118*, 12989–12996.

(6) Nicolet, Y.; Piras, C.; Legrand, P.; Hatchikian, C.; Fontecilla-Camps, J. C. *Structure* **1999**, *7*, 13–23.

(7) Jones, A. K.; Sillery, E.; Albracht, S. P. J.; Armstrong, F. A. *Chem. Commun.* **2002**, 866–867.

(8) Martin, W.; Mueller, M. *Nature* **1998**, *392*, 37–41.

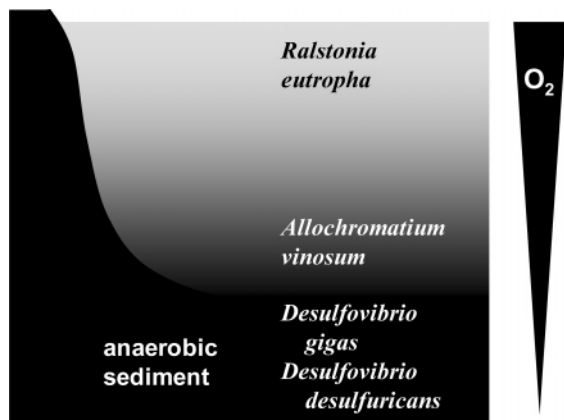


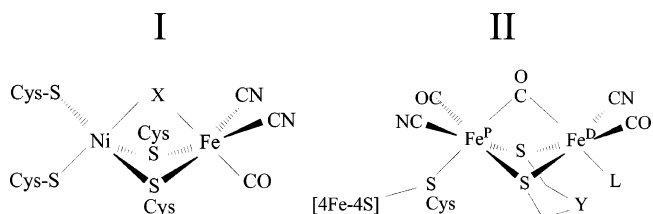
**Figure 1.** Schematic representation of the distribution of hydrogenase-producing microorganisms in a pond, and the extent to which these organisms are likely to be exposed to  $O_2$ . Adapted from refs 1 and 15.

Here we employ direct electrochemical methods, “protein film voltammetry”,<sup>9,10</sup> to compare in detail the effects of an oxidizing potential or  $O_2$  itself on different hydrogenases. This is possible because hydrogenases exhibit fast electron exchange and high catalytic activity when adsorbed on a pyrolytic graphite “edge” (PGE) electrode.<sup>11–14</sup> Catalytic activity is directly recorded as current, thus the status of enzyme molecules adsorbed on the electrode can be studied as a function of potential, and the kinetics of interconversions between active and inactive states can be extracted following initiation of reactions by potential steps or injections of gases.<sup>10,13,14</sup> Very small quantities of enzyme ( $\ll 1$  pmol) can be manipulated, and due to regenerative recycling, multiple consecutive experiments can be carried on a single sample.

We have examined hydrogenases isolated from  $\beta$ -,  $\gamma$ -, and  $\delta$ -proteobacteria derived from different environments, allowing us to formulate a multifaceted definition for tolerance to  $O_2$  and elevated anaerobic oxidizing conditions. The diagram in Figure 1 shows a virtual ‘pond’ representing a spectrum of environments in which hydrogenase-containing microorganisms exist.<sup>15</sup> At the top of the pond is the strictly aerobic respiratory Knallgas bacterium *Ralstonia eutropha* (*Re*), which oxidizes  $H_2$  at ambient levels of  $O_2$ .<sup>16,17</sup> *Re* produces three [NiFe]-hydrogenases, but we consider here only the “uptake” membrane-bound hydrogenase (*Re* [NiFe]-MBH).<sup>18</sup> In the transition zone between aerobic and anaerobic conditions, but still at levels reached by light, is the photosynthetic purple sulfur bacterium

*Allochromatium vinosum* (*Av*), from which we also consider a [NiFe]-hydrogenase.<sup>19</sup> In the anaerobic sediment at the bottom of the pond are the sulfate-reducing bacteria *Desulfovibrio gigas* (*Dg*) and *Desulfovibrio desulfuricans* ATCC 7757 (*Dd*). While these are anaerobes and are, therefore, likely to produce very  $O_2$ -sensitive hydrogenases, *Desulfovibrio* cultures are known to survive temporary exposure to  $O_2$ .<sup>20,21</sup> Here we consider a [NiFe]-hydrogenase from *D. gigas* and an [FeFe]-hydrogenase from *D. desulfuricans* ATCC 7757 (*Dd*).<sup>6,22</sup>

All four hydrogenases are two-subunit enzymes, and in their native state, they are either periplasmic (*Dd* [FeFe]-hydrogenase and *Dg* [NiFe]-hydrogenase) or tightly bound to the periplasmic side of the cytoplasmic membrane (*Av* [NiFe]-hydrogenase and *Re* [NiFe]-MBH).<sup>1</sup> A combination of X-ray crystallographic and FTIR methods applied to purified [NiFe]-hydrogenases from *Av*,<sup>23</sup> *Dg*,<sup>5,24</sup> *Desulfovibrio vulgaris* (Miyazaki F),<sup>25</sup> and *Desulfovibrio fructosovorans*<sup>24,26</sup> has revealed the general architecture of the active sites of [NiFe]-hydrogenases as a bimetallic Ni–Fe center within the larger subunit, in which the metals are bridged by two cysteine sulfur ligands (**I**).<sup>27</sup> The Fe additionally coordinates two  $CN^-$  and one CO ligand, and at the Ni, there are two terminal cysteine ligands. The Ni–Fe center is deeply buried but “wired” to the protein surface by a series of three Fe–S clusters. Crystallographic experiments involving Xe infusion into crystals of the *D. fructosovorans* [NiFe]-hydrogenase have indicated routes for transport of gaseous molecules through the protein.<sup>28</sup>



It is well established that exposure of many [NiFe]-hydrogenases to  $O_2$  leads to varying proportions of two oxidized, inactive states termed Ready ( $Ni-B$  or  $Ni_r^*$ ) and Unready ( $Ni-A$  or  $Ni_u^*$ ).<sup>14,29,30</sup> Each contains Ni(III) and Fe(II), and

- (9) Léger, C.; Elliott, S. J.; Hoke, K. R.; Jeuken, L. J. C.; Jones, A. K.; Armstrong, F. A. *Biochemistry* **2003**, *42*, 8653–8662.  
 (10) Vincent, K. A.; Armstrong, F. A. *Inorg. Chem.* **2005**, *44*, 798–809.  
 (11) Pershad, H. R.; Duff, J. L. C.; Heering, H. A.; Duin, E. C.; Albracht, S. P. J.; Armstrong, F. A. *Biochemistry* **1999**, *38*, 8992–8999. Lamle, S. E.; Vincent, K. A.; Halliwell, L. M.; Albracht, S. P. J.; Armstrong, F. A. *Dalton Trans.* **2003**, 4152–4157.  
 (12) Léger, C.; Jones, A. K.; Roseboom, W.; Albracht, S. P. J.; Armstrong, F. A. *Biochemistry* **2002**, *41*, 15736–15746.  
 (13) Jones, A. K.; Lamle, S. E.; Pershad, H. R.; Vincent, K. A.; Albracht, S. P. J.; Armstrong, F. A. *J. Am. Chem. Soc.* **2003**, *125*, 8505–8514.  
 (14) Lamle, S. E.; Albracht, S. P. J.; Armstrong, F. A. *J. Am. Chem. Soc.* **2004**, *126*, 14899–14909. Lamle, S. E.; Albracht, S. P. J.; Armstrong, F. A. *J. Am. Chem. Soc.* **2005**, *127*, 6595–6604.  
 (15) Schlegel, H. G. *Allgemeine Mikrobiologie*; Thieme Georg Verlag: Stuttgart, 1992; pp 566 and 569.  
 (16) Schwartz, E.; Friedrich, B. The  $H_2$ -Metabolizing Prokaryotes. In *The Prokaryotes: An Evolving Electronic Resource for the Microbiological Community*, 3rd ed. (release 3.14); Dworkin, M., Schleifer, K. H., Stackebrandt, E., Eds.; Springer: New York, 2003.  
 (17) Schink, B.; Probst, I. *Biochem. Biophys. Res. Commun.* **1980**, *95*, 1563–1569.  
 (18) Schink, B.; Schlegel, H. G. *Biochim. Biophys. Acta* **1979**, *567*, 315–324.

- (19) This enzyme is now also considered to be membrane bound and is referred to as MBH by some authors (e.g., ref 31).  
 (20) Cypionka, H. *Annu. Rev. Microbiol.* **2000**, *54*, 827–848.  
 (21) Baumgarten, A.; Redenius, I.; Kranczoch, J.; Cypionka, H. *Arch. Microbiol.* **2001**, *176*, 306–309. Fareleira, P.; Santos, B. S.; Antonio, C.; Moradas-Ferreira, P.; LeGall, J.; Xavier, A. V.; Santos, H. *Microbiology* **2003**, *149*, 1513–1522.  
 (22) Hatchikian, C.; Forget, N.; Fernandez, V. M.; Williams, R.; Cammack, R. *Eur. J. Biochem.* **1992**, *209*, 357–365.  
 (23) Bagley, K. A.; Van Garderen, C. J.; Chen, M.; Duin, E. C.; Albracht, S. P. J.; Woodruff, W. H. *Biochemistry* **1994**, *33*, 9229–9236. Bagley, K. A.; Duin, E. C.; Roseboom, W.; Albracht, S. P. J.; Woodruff, W. H. *Biochemistry* **1995**, *34*, 5527–5535. Happe, R. P.; Roseboom, W.; Pierik, A. J.; Albracht, S. P. J.; Bagley, K. A. *Nature* **1997**, *385*, 126.  
 (24) Volbeda, A.; Martin, L.; Cavazza, C.; Matho, M.; Faber, B. W.; Roseboom, W.; Albracht, S. P. J.; Garcin, E.; Rousset, M.; Fontecilla-Camps, J. C. *J. Biol. Inorg. Chem.* **2005**, *10*, 239–249.  
 (25) Higuchi, Y.; Yagi, T.; Yasuoka, N. *Structure* **1997**, *5*, 1671–1680. van Gastel, M.; Fichtner, C.; Neese, F.; Lubitz, W. *Biochem. Soc. Trans.* **2005**, *33*, 7–11.  
 (26) Volbeda, A.; Montet, Y.; Vermede, X.; Hatchikian, E. C.; Fontecilla-Camps, J. C. *Int. J. Hydrogen Energy* **2002**, *27*, 1449–1461.  
 (27) Albracht, S. P. J. *Biochim. Biophys. Acta* **1994**, *1188*, 167–204.  
 (28) Montet, Y.; Amara, P.; Volbeda, A.; Vermede, X.; Hatchikian, E. C.; Field, M. J.; Frey, M.; Fontecilla-Camps, J. C. *Nat. Struct. Biol.* **1997**, *4*, 523–526.  
 (29) Fernandez, V. M.; Hatchikian, E. C.; Cammack, R. *Biochem. Biophys. Acta* **1985**, *832*, 69–79.  
 (30) Happe, R. P.; Roseboom, W.; Albracht, S. P. J. *Eur. J. Biochem.* **1999**, *259*, 602–608.

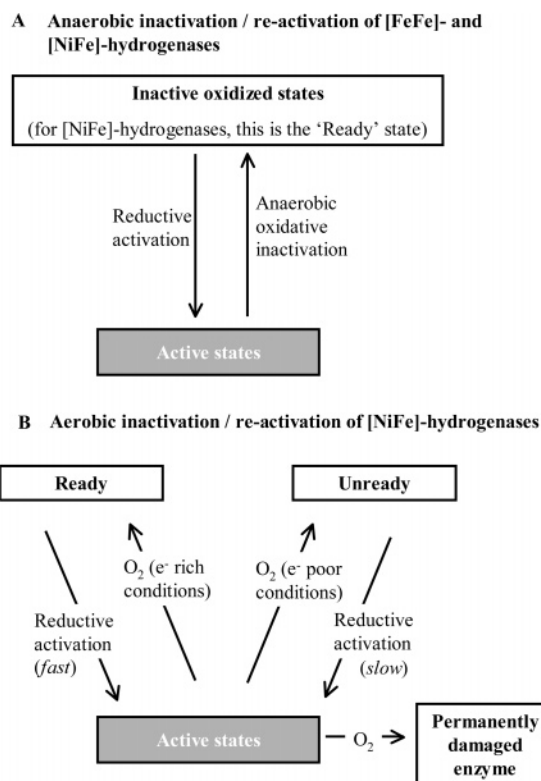


**Figure 2.** (A) Interconversion between active and oxidized, inactive states of [FeFe]- or [NiFe]-hydrogenases under anaerobic conditions. (B) Reactions of [NiFe]-hydrogenases with  $O_2$  to generate inactive states that can be reactivated, at least to some extent, by reductive activation. The formation of Unready and Ready states is well-characterized for [NiFe]-hydrogenases from *D. gigas*, *A. vinosum*, and *Desulfovibrio fructosovorans*.<sup>14,24,27,29</sup>

they are distinguished on the basis of the rates of their reductive reactivation to regenerate catalytically active forms of the enzyme and on their corresponding spectral properties<sup>29,31</sup> (Figure 2B). Anaerobic oxidation also generates the Ready state (Figure 2A). Crystallographic studies of the Ready and Unready forms of *D. gigas* [NiFe]-hydrogenase have shown the presence of a bridging ligand (X) between the Ni and Fe sites that initially appeared to be a hydroxide in both states. Thus, the structural basis for the kinetic difference between the Ready and Unready states has long been a puzzle.<sup>27</sup> However, recent electrochemical results<sup>14</sup> and re-evaluation of X-ray crystallographic data<sup>24</sup> have provided an answer, suggesting that the Unready state of *Av* and *Dg* [NiFe]-hydrogenase contains a partially reduced  $O_2$  species, probably peroxide in a bridging position, and that only the Ready state has a hydroxide bridge (see note added in proof).

Although [FeFe]-hydrogenases share no sequence homology with the [NiFe]-enzymes and probably evolved separately,<sup>1</sup> there are remarkable parallels in their active-site structures and reactions. Crystallographic and FTIR studies on the [FeFe]-hydrogenases from *D. vulgaris*,<sup>32</sup> *D. desulfuricans*,<sup>6,33</sup> and *Clostridium pasteurianum*<sup>34</sup> reveal that each Fe coordinates two

diatomic ligands (probably one CO and one  $CN^-$ ), and that in addition to a bridging CO, a non-peptide bridge, possibly a 1,3-propanedithiolate or a di(thiomethyl)amine, links the Fe sites.<sup>35</sup> A minimal structure representation (II) is shown. The catalytic states are tentatively assigned as Fe(II)Fe(I) and Fe(I)Fe(I).<sup>33,36,37</sup> A [4Fe–4S] cluster is linked to one active-site Fe (called  $Fe^P$ , the proximal site, as opposed to  $Fe^D$ , the distal site) via a bridging cysteine, forming part of an electron-transfer chain of Fe–S clusters that wires the active site to the surface of the protein as in the [NiFe]-hydrogenases. Putative gas channels have also been found in the *Dd* [FeFe]-hydrogenase.<sup>6</sup> Like its [NiFe]- counterparts from *Desulfovibrio* species, the [FeFe]-hydrogenase from *D. desulfuricans* ATCC 7757 can be purified aerobically; however, the as-isolated enzyme is in an inactive state.<sup>6,22</sup> It has been shown for the *D. vulgaris* (Hildenborough) [FeFe]-hydrogenase (which has complete amino acid sequence identity to the *D. desulfuricans* enzyme<sup>38</sup>) that the reductively activated enzyme (Figure 2A) becomes highly sensitive to  $O_2$ .<sup>39–41</sup>

This paper describes a new strategy for comparing, quantitatively, the tolerance of hydrogenases to  $O_2$  and oxidizing conditions.

## Methods

Experiments were carried out in a glovebox (MBraun or Vacuum Atmospheres) maintained at  $<2$  ppm  $O_2$  (see below). Pyrolytic graphite edge (PGE) electrodes were constructed as described previously and polished with an aqueous slurry of 1.0  $\mu m$  alumina prior to use.<sup>13</sup> Electrode rotation (typically 2500 rpm) was controlled by an EG&G M636 electrode rotator. The glass electrochemical cell incorporated a platinum counter electrode and, as the reference, an isolated saturated calomel electrode (SCE) held in a Luggin sidearm containing 0.1 M NaCl. All potentials are quoted versus the standard hydrogen electrode (SHE); we have used  $E_{SHE} = E_{SCE} + 241$  mV at 25 °C.<sup>42</sup> The cell was fitted with a septum for injection of liquids into the cell solution, a water jacket for temperature control, and gas inlet and outlet valves. All experiments were performed with either  $H_2$  (Premier Grade, Air Products) or  $N_2$  (Oxygen Free, BOC) flushing through the headspace above the cell solution. Stock solutions of  $O_2$ -saturated buffer were prepared by taking a portion of the pH-adjusted buffer in a vial sealed with a septum and flushing with  $O_2$  (Air Products) for 5 min.

*Av* [NiFe]-hydrogenase,<sup>43</sup> *Re* [NiFe]-MBH,<sup>44</sup> *Dg* [NiFe]-hydrogenase,<sup>45</sup> and *Dd* [FeFe]-hydrogenase<sup>22</sup> were purified as described previously. A mixed buffer system was used in all experiments; this consisted of 15 mM in each of sodium acetate, MES (2-[*N*'-morpholino]ethane sulfonic acid), HEPES (*N*'-[2-hydroxyethyl]piperazine-*N*'-2-ethane sulfonic acid), TAPS (*N*'-tris[hydroxymethyl]methyl-3-amino propane sulfonic acid), and CHES (2-[*N*'-cyclohexylamino]ethane

- (31) Bleijlevens, B.; van Broekhuizen, F. A.; Lacey, A. L.; Roseboom, W.; Fernandez, V. M.; Albracht, S. P. J. *J. Biol. Inorg. Chem.* **2004**, *9*, 743–752.  
 (32) van der Spek, T. M.; Arendsen, A. F.; Happe, R. P.; Yun, S. Y.; Bagley, K. A.; Stufkens, D. J.; Hagen, W. R.; Albracht, S. P. J. *Eur. J. Biochem.* **1996**, *237*, 629–634. Pierik, A. J.; Hulstein, M.; Hagen, W. R.; Albracht, S. P. J. *Eur. J. Biochem.* **1998**, *258*, 572–578.  
 (33) De Lacey, A. L.; Stadler, C.; Cavazza, C.; Hatchikian, C.; Fernandez, V. M. *J. Am. Chem. Soc.* **2000**, *122*, 11232–11233.  
 (34) Peters, J. W.; Lanzilotta, W. N.; Lemon, B. J.; Seefeldt, L. C. *Science* **1998**, *282*, 1853–1858.

- (35) Nicolet, Y.; De Lacey, A. L.; Venede, X.; Fernandez, V. M.; Hatchikian, E. C.; Fontecilla-Camps, J. C. *J. Am. Chem. Soc.* **2001**, *123*, 1596–1601.  
 (36) Armstrong, F. A. *Curr. Opin. Chem. Biol.* **2004**, *8*, 133–140.  
 (37) Liu, Z.-P.; Hu, P. *J. Am. Chem. Soc.* **2002**, *124*, 5175–5182.  
 (38) Hatchikian, E. C.; Magro, V.; Forget, N.; Nicolet, Y.; Fontecilla-Camps, J. C. *J. Bacteriol.* **1999**, *181*, 2947–2952.  
 (39) Van der Westen, H. M.; Mayhew, S. G.; Veeger, C. *FEBS Lett.* **1978**, *86*, 122–126.  
 (40) Pierik, A. J.; Hagen, W. R.; Redeker, J. S.; Wolbert, R. B. G.; Boersma, M.; Verhagen, M. F. J. M.; Grande, H. J.; Veeger, C.; Mutsaers, P. H. A.; Sands, R. H.; Dunham, W. R. *Eur. J. Biochem.* **1992**, *209*, 63–72.  
 (41) Dijk, C.; Van Berkel-Arts, A.; Veeger, C. *FEBS Lett.* **1983**, *156*, 340–344.  
 (42) Bard, A. J.; Faulkner, L. R. *Electrochemical Methods. Fundamentals and Applications*, 2nd ed.; Wiley: New York, 2001.  
 (43) Coremans, J. M. C. C.; Van der Zwaan, J. W.; Albracht, S. P. J. *Biochim. Biophys. Acta* **1992**, *1119*, 157–168.  
 (44) The purification of *R. eutropha* [NiFe]-MBH will be published elsewhere.  
 (45) Hatchikian, E. C.; Bruschi, M.; Le Gall, J. *Biochem. Biophys. Res. Commun.* **1978**, *82*, 451–461.

sulfonic acid) (all from Sigma), with 0.1 M NaCl as supporting electrolyte. All solutions were prepared using purified water (Millipore: 18 M $\Omega$  cm) and titrated with NaOH or HCl to pH 6.0 at 30 °C.

We have described previously how the *Av* [NiFe]-hydrogenase may be studied by protein film voltammetry.<sup>11–14</sup> The enzyme adsorbs from dilute enzyme solution (containing 0.2 mg mL<sup>-1</sup> polymyxin B sulfate as coadsorbate) onto a freshly polished graphite electrode, as the potential is cycled between -558 and +242 mV at 10 mV s<sup>-1</sup> over a period of about 30 min. This procedure gives a submonolayer film of high electrocatalytic activity. The electrode is then rinsed and placed in the electrochemical cell containing 2 mL of pristine mixed buffer. Importantly, no enzyme is added to this solution so that protein molecules that have not been subjected to potential control do not exchange with molecules adsorbed on the electrode and complicate interpretation of results. While this obviously gives rise to a film that is inherently unstable and protein molecules will slowly desorb, this configuration not only optimizes potential control over the chemistry taking place but also ensures that addition of O<sub>2</sub> (or indeed any reagent) to the cell causes reaction with only a tiny, trapped population of enzyme (10–100 fmol). The method is thus also extremely economical in terms of sample requirement. Films of the *Dg* [NiFe]-hydrogenase or *Dd* [FeFe]-hydrogenase were formed in a similar manner. Films of *Re* [NiFe]-MBH were prepared by spotting 1.5  $\mu$ L of dilute enzyme solution (containing no polymyxin B sulfate) onto the freshly polished graphite surface and then withdrawing the solution with a pipet before placing the electrode into the buffered cell solution (also without polymyxin B sulfate as this was found to destabilize the film). All films were prepared at room temperature, but experiments were carried out at 30 °C. The pH of a sample of the cell solution was checked at 30 °C after each experiment. Following adsorption onto the electrode and between experiments, reductive activation of the hydrogenases was achieved by poisoning the potential at -558 mV with H<sub>2</sub> in the cell, typically for 1 h at 45 °C for the *Av* and *Dg* [NiFe]-hydrogenases (to bring the rate of reactivation into a reasonable time frame), and for 5 min at 30 °C for the *Re* [NiFe]-MBH and the *Dd* [FeFe]-hydrogenase. These activation steps were usually implemented in addition to the steps carried out as part of the experiments discussed in the text. Experiments with the *Dd* [FeFe]-hydrogenase were carried out with a cell encased in black tape to minimize possible light effects.<sup>46</sup>

## Results and Discussion

**Catalytic Bias: H<sub>2</sub> Oxidation versus H<sup>+</sup> Reduction.** Figure 3 shows cyclic voltammograms for the four hydrogenases considered in this study, measured under identical conditions: 30 °C, pH 6 and 1 bar H<sub>2</sub>. These experiments compare the behavior under anaerobic conditions and thus probe reactions that are probably analogous to those occurring with cellular electron acceptors and donors other than O<sub>2</sub>. By anaerobic conditions, we mean that the O<sub>2</sub> level is not above 2 ppm, that is, approximately 10<sup>-9</sup> M, but we note that this would still be far above that corresponding to stoichiometry with the adsorbed sample on the electrode.<sup>47</sup>

The voltammograms shown in Figure 3A were recorded at scan rates of  $\geq 100$  mV s<sup>-1</sup>. Scans in gray show the response of the blank electrode without adsorbed protein, while black lines show the behavior of the hydrogenase films. The electrode was first poised at a potential (*E*) of -558 mV to ensure

complete reductive activation of each enzyme film and then swept to high potential and back to -558 mV. We consider first the results for the [FeFe]-hydrogenase from *Desulfovibrio desulfuricans*, an organism from the sediment of the pond. For this enzyme, there is a large negative current (*i*) at the most negative potentials due to electrocatalytic proton reduction (H<sub>2</sub> evolution). As the potential is swept in a positive direction, the rate of proton reduction decreases and the rate of H<sub>2</sub> oxidation increases so that a positive current is recorded at high potentials.<sup>48</sup> The appearance of the voltammogram gives an excellent indication of the bias of the enzyme toward H<sup>+</sup> reduction versus H<sub>2</sub> oxidation; thus we see immediately that the [FeFe]-hydrogenase is a good H<sub>2</sub>-evolution catalyst even at 1 bar H<sub>2</sub>. Confirmation that the negative current is due to H<sub>2</sub> evolution comes from two observations, the first of which is made when the experiment is carried out under N<sub>2</sub> instead of H<sub>2</sub> (Figure 4). In the first scan, the electrode is stationary and H<sub>2</sub> produced at low potentials is re-oxidized at more positive potentials, giving rise to a positive current peak. In the second scan, the electrode is rotated so that the H<sub>2</sub> produced at low potentials is spun away; the positive current response at more positive potentials is now absent, as there is no H<sub>2</sub> available to be oxidized.

The second observation (returning to Figure 3) concerns the potential at which the current changes from negative to positive (averaged for the forward and reverse scans), which is the potential of zero net current: this value corresponds to the formal reduction potential of the 2H<sup>+</sup>/H<sub>2</sub> couple expected under these conditions (-360 mV at pH 6, 30 °C, 1 bar H<sub>2</sub>) and is marked by a dashed vertical line in each panel.

In the simplest case, a plateau should be reached when the catalysis becomes controlled by the chemistry of the active site rather than by interfacial electron transfer driven by the electrode potential.<sup>49</sup> In most cases this is not the case, and a residual slope is observed—the enzymes are so active that interfacial electron transfer is probably limiting.<sup>49</sup> Provided the catalyst remains fully active, this shape is retraced on the reverse scan, offset by non-Faradaic contributions (often small) from the charging of the electrode (seen in the scans performed without enzyme on the electrode). All the hydrogenases inactivate reversibly at high potentials, as discussed below, but this is much more rapid for *Dd* [FeFe]-hydrogenase; hence, it is observed even at 200 mV s<sup>-1</sup>.

In contrast to *Dd* [FeFe]-hydrogenase, the [NiFe] enzymes show very low or zero H<sup>+</sup> reduction activity (Figure 3). This lack of activity is mainly due to inhibition of this reaction by H<sub>2</sub> since significant H<sup>+</sup> reduction currents are observed under an inert N<sub>2</sub> atmosphere.<sup>12</sup> For the *Av* and *Dg* [NiFe]-hydrogenases, the onset potential for electrocatalytic H<sub>2</sub> oxidation is close to -360 mV, whereas with *Re* [NiFe]-MBH, for which a H<sup>+</sup> reduction current is not detectable at 1 bar H<sub>2</sub>, the onset of H<sub>2</sub> oxidation is shifted to more positive potential by about 80 mV.

(46) Patil, D. S.; He, S. H.; DerVartanian, D. V.; Le Gall, J.; Huynh, B. H.; Peck Jr., H. D. *FEBS Lett.* **1988**, *228*, 85–88.

(47) We assume an upper limit of 1 pmol cm<sup>-2</sup> for enzyme coverage on the electrode of surface area 0.03 cm<sup>2</sup>; this corresponds to an effective concentration of just 2  $\times$  10<sup>-11</sup> M if all adsorbed sample was released into solution; that is, there could be a 50-fold excess of O<sub>2</sub>. Furthermore, during measurements at low potentials, O<sub>2</sub> is evolved at the counter electrode. We are currently designing even more rigorous experiments to address these issues.

(48) It is important to note the significance of such rapid electrocatalysis that greatly amplifies the electrochemical response of so few enzyme molecules (normally below the detection limit of ca. 1 pmol cm<sup>-2</sup> under non-turnover conditions). For example, during the voltammogram shown in Figure 3B, each molecule of *A. vinosum* [NiFe]-hydrogenase undergoes approximately 3 million turnover cycles (assuming an electroactive coverage of ca. 1 pmol cm<sup>-2</sup>).

(49) Léger, C.; Jones, A. K.; Albracht, S. P. J.; Armstrong, F. A. *J. Phys. Chem. B* **2002**, *106*, 13058–13063.

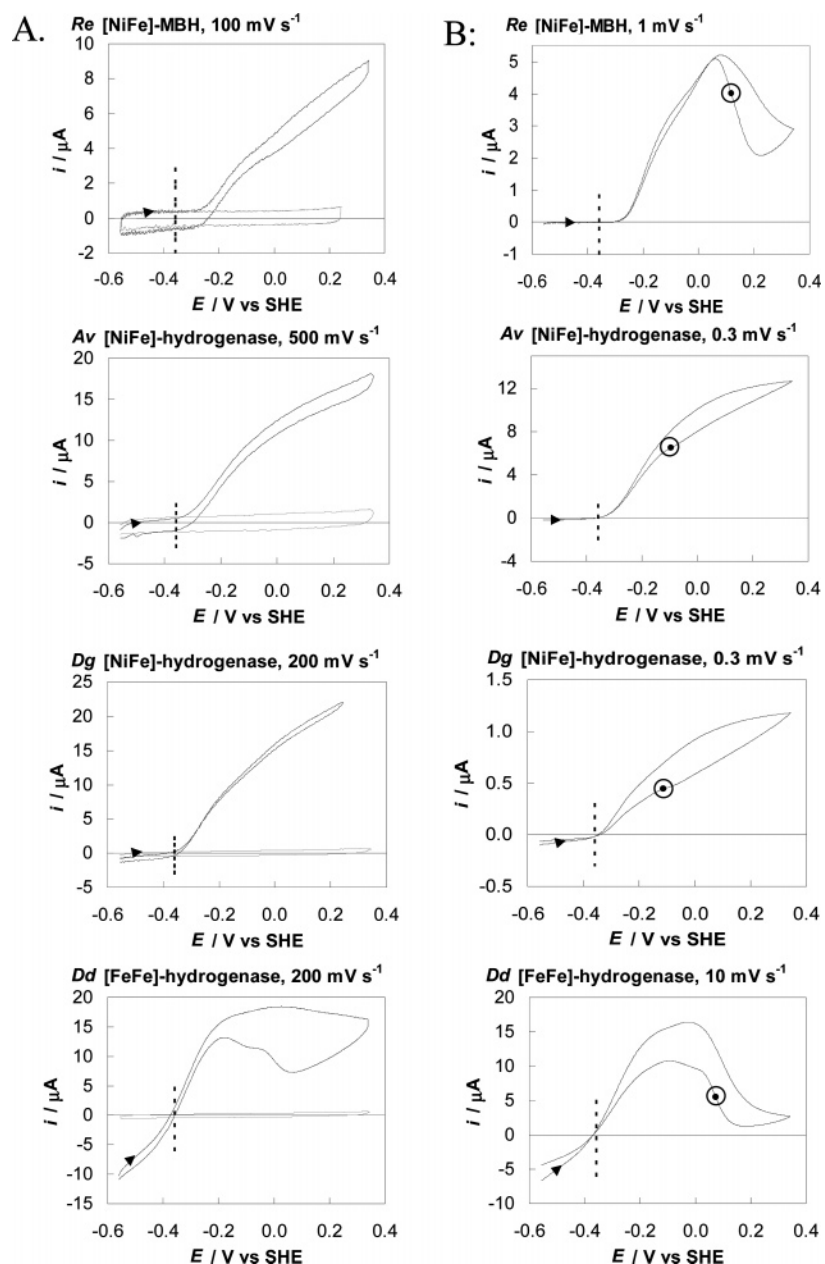


**Figure 3.** Cyclic voltammograms recorded at a PGE electrode rotated at 2500 rpm, under anaerobic conditions at 1 bar  $H_2$ , pH 6, 30 °C. All panels are ladderred with the same potential scale to aid comparison. Included in (A) are the voltammetric responses for a bare electrode. The voltammograms show the response for a film of adsorbed hydrogenase (*Ralstonia eutropha*, *Re*; *Allochroamatium vinosum*, *Av*; *Desulfovibrio gigas*, *Dg*; *Desulfovibrio desulfuricans*, *Dd*). Scan rates in (A) have been selected, where possible, to outrun oxidative inactivation. In (B), scan rates have been chosen to reveal oxidative inactivation and reductive reactivation, and the switch potentials (see text) are indicated by a dot (circled). Dashed vertical lines indicate the potential of the  $H^+/H_2$  couple under the experimental conditions, and arrows indicate the direction of the scan.

**Anaerobic Oxidative Inactivation and Reductive Reactivation.** Figure 3B shows voltammograms also recorded at 1 bar  $H_2$ , but now at slower scan rates so that we can observe how the enzymes inactivate and reactivate under anaerobic conditions at high potentials. At the slower scan rates employed here, loss of enzyme from the electrode during the experiment is evident, resulting in lower currents on the return scans.<sup>50</sup> At 1  $mV s^{-1}$ , the  $H_2$  oxidation activity of the *Re* [NiFe]-MBH is “switched off” as the electrode is swept to potentials above about +50 mV (leading to a drop in catalytic current). The  $H_2$

oxidation activity is restored during the return scan by reductive activation. Anaerobic inactivation is sufficiently slow for the *Av* and *Dg* hydrogenases that relatively little inactivation occurs during the cycle even at 0.3  $mV s^{-1}$ ; reductive reactivation (Figure 3B) is evident only as a slight inflection in the trace at about  $-100$  mV. The “switch” potential ( $E_{switch}$ ) associated with anaerobic inactivation/reactivation has been defined previously as the steepest point of the current ascent during reductive activation, obtained by taking the derivative  $di/dE$ .<sup>13</sup> We have already explored high-potential inactivation and reactivation in detail for the *Av* enzyme,<sup>13</sup> showing that the high-potential inactivation observed electrochemically is consistent with

(50) However, these experiments focus on the measurement of potentials controlling catalytic activity, and the potentials do not vary between films of different coverage.

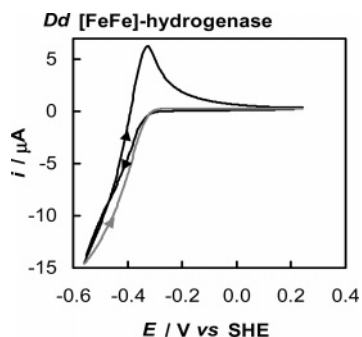


**Figure 4.** Voltammograms recorded at a PGE electrode coated with *D. desulfuricans* [FeFe]-hydrogenase at  $10 \text{ mV s}^{-1}$  (pH 6,  $25^\circ \text{C}$  and under  $\text{N}_2$ ). In the first cycle (black line) the electrode was stationary, while in the second scan (gray line) the electrode was rotated at 200 rpm.

generation of an inactive form of the enzyme known as the Ready state (Figure 2A) that has been well-characterized through spectroscopic experiments.<sup>27,29,51</sup> In the absence of detailed spectroscopic studies, it is unclear whether the form of the *Re* [NiFe]-MBH generated by anaerobic oxidative inactivation corresponds structurally to the Ready state of the *Av* and *Dg* [NiFe]-hydrogenases. The cyclic voltammogram for the *Dd* [FeFe]-hydrogenase shows that this enzyme also converts to an inactive state at high potentials and reactivates rapidly on the reverse potential sweep. Under these conditions, anaerobic inactivation and reactivation are so rapid that these processes proceed almost to completion even in a voltammogram recorded at  $10 \text{ mV s}^{-1}$ .

Some additional features (multiple current maxima) are evident in many of these voltammograms; these are under investigation and will be analyzed in further papers.<sup>52</sup>

**Inactivation by  $\text{O}_2$ .** We turn our attention next to aerobic conditions, first considering the effects of  $\text{O}_2$  on the [NiFe]-hydrogenases. The cyclic voltammograms for the *Re*, *Av*, and *Dg* [NiFe]-hydrogenases (Figure 5) were recorded at  $1 \text{ mV s}^{-1}$ , during which, at approximately 0 mV on the forward sweep,  $200 \mu\text{L}$  of  $\text{O}_2$ -saturated buffer was injected into the 2 mL cell solution (corresponding to an  $\text{O}_2$  concentration of ca.  $90 \mu\text{M}$ ). The injection potential was chosen such that  $\text{O}_2$  was not present in solution at potentials causing its reduction at the electrode. The  $\text{O}_2$  was then removed by flushing the headspace of the cell with  $\text{H}_2$  throughout the remainder of the voltammetric scan. From control experiments, in which  $\text{O}_2$  reduction is monitored at a bare graphite electrode poised at low potential, we estimate that removal of  $\text{O}_2$  is complete approximately 5 min after the injection, corresponding to a 300 mV interval at  $1 \text{ mV s}^{-1}$ . Thus  $\text{O}_2$  removal is complete by the time of reversal of scan direction at +342 mV in the voltammograms shown in Figure 5.

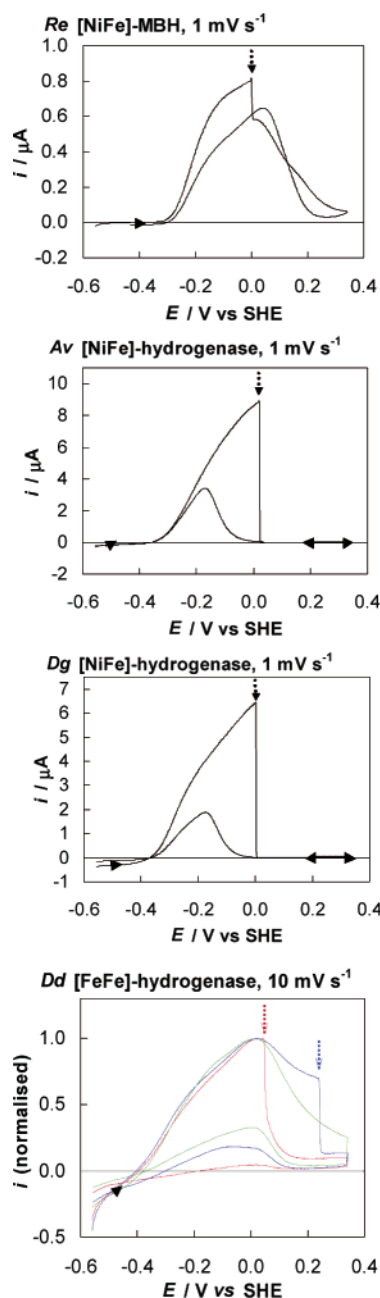


**Figure 5.** Cyclic voltammograms recorded at  $1 \text{ mV s}^{-1}$  for the *R. eutropha* (*Re*) [NiFe]-MBH and *A. vinosum* (*Av*) and *D. gigas* (*Dg*) [NiFe]-hydrogenases. At 0 mV on the oxidative sweep,  $\text{O}_2$ -saturated buffer was injected (indicated by a dashed arrow) and then rapidly removed by flushing the headspace in the electrochemical cell with  $\text{H}_2$ . Three voltammograms are shown for the *D. desulfuricans* (*Dd*) [FeFe]-hydrogenase; these were recorded at  $10 \text{ mV s}^{-1}$  with a 300 s pause at +342 mV before the return sweep toward more negative potentials. Red line:  $\text{O}_2$  injected at +42 mV. Blue line:  $\text{O}_2$  injected at +242 mV. Green line: anaerobic cycle. Each  $\text{O}_2$  injection involved introduction of  $200 \mu\text{L}$  of  $\text{O}_2$ -saturated buffer into a 2 mL cell solution, resulting in ca.  $90 \mu\text{M}$  [ $\text{O}_2$ ] in the cell solution, which was then flushed out over the following 300 s. Other conditions were: pH 6,  $30^\circ \text{C}$ , 1 bar  $\text{H}_2$ , electrode rotation at 2500 rpm. Solid arrows indicate the direction(s) of scan.

The voltammograms show immediately that  $\text{O}_2$  affects the activity of all three [NiFe]-hydrogenases. The catalytic current drops very rapidly to zero for the *Av* and *Dg* enzymes, indicating complete inhibition by  $\text{O}_2$ . In contrast, the current drops by only 30% when *Re* [NiFe]-MBH is exposed to  $90 \mu\text{M}$   $\text{O}_2$ , establishing clearly that this enzyme continues to catalyze  $\text{H}_2$  oxidation

(51) Fernandez, V. M.; Hatchikian, E. C.; Patil, D. S.; Cammack, R. *Biochim. Biophys. Acta* **1986**, 883, 145–154. Bleijlevens, B. The hydrogen-consumption activity of the [NiFe] hydrogenase of *Allochromatium vinosum* in different redox states. In *Hydrogen as a Fuel, Learning from Nature*; Cammack, R., Frey, M., Robson, R., Eds.; Taylor & Francis: London, 2001; pp 82–84. De Lacey, A. L.; Hatchikian, E. C.; Volbeda, A.; Frey, M.; Fontecilla-Camps, J. C.; Fernandez, V. M. *J. Am. Chem. Soc.* **1997**, 119, 7181–7189.

(52) In a recent study of the catalytic electron transport mechanism of *E. coli* fumarate reductase (Hudson, J. M.; Heffron, K.; Kotlyar, V.; Sher, Y.; Maklashina, E.; Cecchini, G.; Armstrong, F. A. *J. Am. Chem. Soc.* **2005**, 127, 6977–6989), we showed that complex features observed in the voltammetry during electrocatalytic fumarate reduction reflected the rates and energetics of electron flow through a specific 4Fe–4S cluster in the enzyme. Voltammograms for native *R. eutropha* MBH (not shown) have the same appearance as that of the *Strep*-tagged MBH shown here, indicating that the features observed are inherent to the enzyme rather than the result of the sample history.

in the presence of  $O_2$ . (The remaining active enzyme is then subject to the high-potential anaerobic inactivation described above.) For the *Av* and *Dg* enzymes, there is no recovery of current at high potentials, even after  $O_2$  has been completely removed from solution, but both enzymes show substantial recovery of activity below 0 mV on the return sweep. The *Re* [NiFe]-MBH begins to recover activity even before removal of  $O_2$  from solution is complete, at potentials more positive than +150 mV.

We next consider the effect of  $O_2$  on the *Dd* [FeFe]-hydrogenase, shown in the lower panel of Figure 5. As mentioned above, it has been observed that as-isolated oxidized inactive [FeFe]-hydrogenase is somehow protected against damage by  $O_2$ ,<sup>39–41</sup> and we have designed experiments in which  $O_2$  is injected at high and low potentials to compare the effects of  $O_2$  on enzyme that has been inactivated anaerobically versus enzyme that is almost fully active. Film instability appears to be a particular problem for the *Dd* [FeFe]-hydrogenase,<sup>53</sup> and to minimize this complication, the  $O_2$  injection experiments were performed at a faster scan rate (10  $mV s^{-1}$ ), with the electrode being poised at +342 mV for 300 s to allow for complete removal of  $O_2$ . For the ensuing discussion, it is important to note that the enzyme is almost fully active at +42 mV prior to injection of  $O_2$  (red line), whereas a substantial portion of the enzyme sample has already converted to the oxidized, inactive form when  $O_2$  is injected at +242 mV (blue line). For comparison, an anaerobic cycle is also shown (green line).<sup>54</sup> First, we note that the current drops essentially to zero upon injection of  $O_2$  at either +42 or +242 mV. Almost no recovery of activity is observed on the return scan after introduction of  $O_2$  at +42 mV, and whereas some reductive reactivation is observed on the return scan after introduction of  $O_2$  at +242 mV, there is still much less recovery than in the anaerobic experiment. (Note though that even in the anaerobic case, the voltammograms lose intensity quite rapidly over the experimental time period.) These experiments provide a quantitative basis for earlier observations suggesting that the inactive, oxidized form of [FeFe]-hydrogenases is unreactive toward  $O_2$  but the active form is irreversibly damaged.<sup>39–41</sup>

We now describe potential sweep and potential step experiments designed to unravel the switch potentials, kinetics, and extent of recovery for each enzyme.

**The Potential Required for Reactivation after Inactivation by  $O_2$ .** Figure 6 shows voltammograms for [NiFe]-hydrogenases following inactivation by  $O_2$ , recorded at sufficiently slow scan rates to obtain an accurate switch potential. These experiments thus report on the *thermodynamics* of reductive reactivation. We did not carry out analogous experiments on the *Dd* [FeFe]-hydrogenase because the inactivation by  $O_2$  could not be reversed on our experimental time scale. In each case, the electrochemical cell was first flushed with  $N_2$ , the electrode potential was stepped to +342 mV, and 200  $\mu L$  of  $O_2$ -saturated buffer was injected; the  $O_2$  was then removed by flushing with  $N_2$  for 5 min, and with  $H_2$  for a further 5 min. The sweeps were therefore performed *anaerobically* at 1 bar  $H_2$  after each

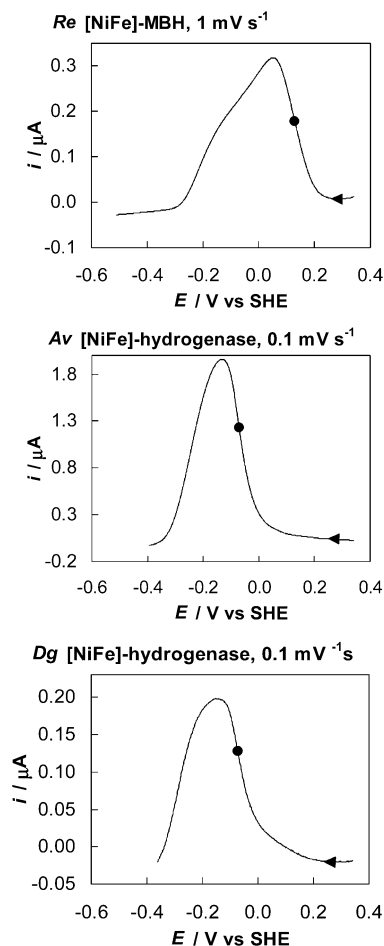


**Figure 6.** Voltammograms showing the reductive activation of [NiFe]-hydrogenases after inactivation with  $O_2$ . Prior to each scan, the electrode was first polarized at  $-558$  mV under 1 bar  $H_2$  to ensure complete activation of the enzyme film. The gas space in the electrochemical cell was then flushed with  $N_2$  for 5 min to remove  $H_2$ . Immediately after a potential step to +342 mV, 200  $\mu L$  of  $O_2$ -saturated buffer was injected into the 2 mL cell solution, and the headspace was flushed with  $N_2$  for 5 min to remove  $O_2$ , and then with  $H_2$  for 5 min. Switch potentials are marked with dots. Other conditions were: pH 6, 30  $^{\circ}C$ , 1 bar  $H_2$ , electrode rotation at 2500 rpm.

enzyme film had experienced a similar pulse of  $O_2$ . Aerobic inactivation of the enzymes was carried out at high potential and under an atmosphere of  $N_2$  because it has been shown for the *Av* [NiFe]-hydrogenase that these conditions lead to generation of predominantly Unready enzyme, which is formed only after exposure to  $O_2$  (Figure 2B).<sup>14</sup> Essentially no anaerobic inactivation was allowed to occur before injection of  $O_2$ , and therefore, the recovery of activity seen during the potential sweeps in Figure 6 clearly represents reactivation of  $O_2$ -inactivated enzyme. For the *Re* [NiFe]-MBH, the potential was swept at 1  $mV s^{-1}$  because recovery is faster than for the other [NiFe]-hydrogenases (see below). The switch potentials are +130 mV (*Re*),  $-70$  mV (*Av*), and  $-75$  mV (*Dg*). Thus the activity of *Re* [NiFe]-MBH begins to recover at +200 mV following exposure to  $O_2$ , whereas the *Av* and *Dg* enzymes remain inactive unless the potential is taken below 0 mV. In practical terms, this means that it is not necessary to have a reductant with a low reduction potential in order to reactivate *Re* [NiFe]-MBH; clearly this enzyme has a much wider potential window for activity under aerobic conditions, even considering the more positive potential required to elicit  $H_2$  oxidation.

(53) We cannot rule out the possibility that damage by traces of  $O_2$  rather than film loss accounts for the decrease in current observed during experiments on this enzyme.

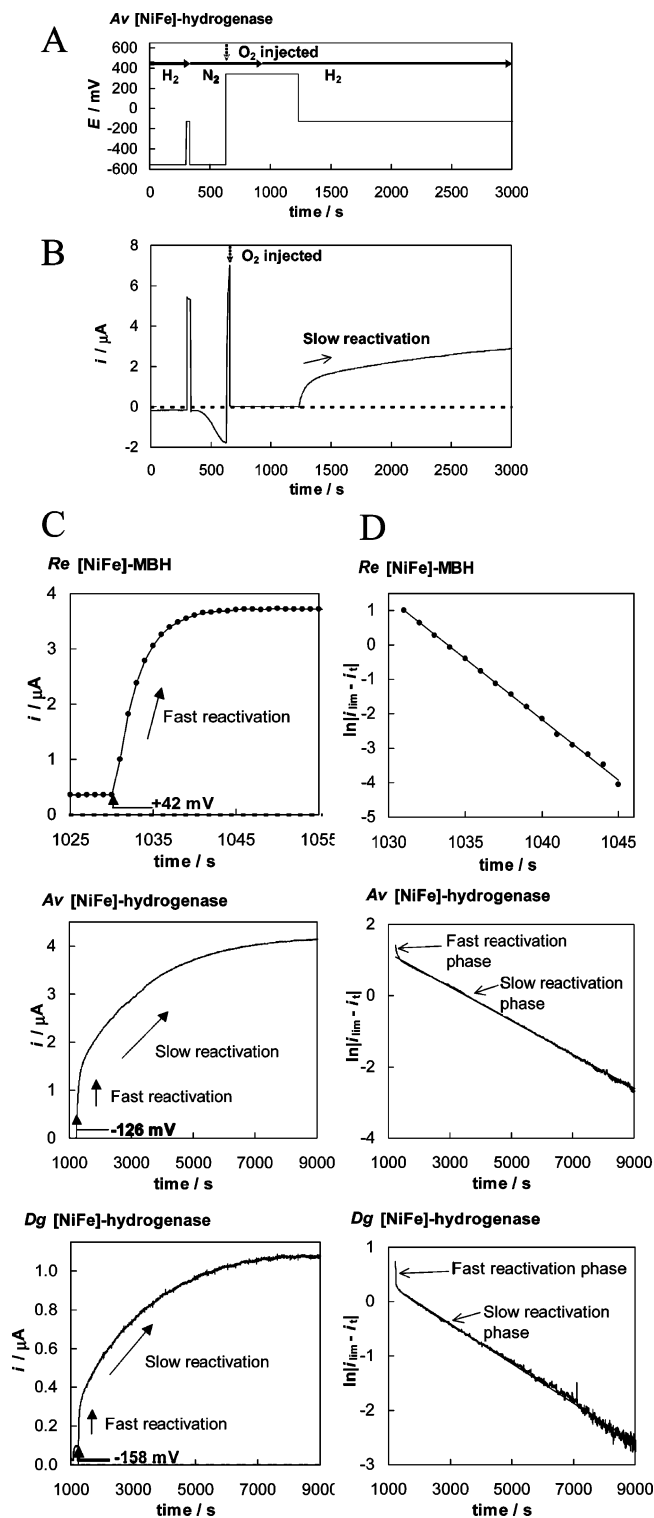
(54) The currents in the cyclic voltammograms for the *Dd* [FeFe]-hydrogenase shown in Figure 5 have been normalized according to the catalytic current at 0 V on the oxidative scan, at which time none of the enzyme samples has been exposed to  $O_2$ .



**The Rate of Reductive Reactivation after Inactivation by O<sub>2</sub>.** We now describe potential-step experiments designed to provide information on the *kinetics* of reductive activation of [NiFe]-hydrogenases after inactivation by O<sub>2</sub>. Reactivation of Unready *Av* [NiFe]-hydrogenase has already been studied electrochemically over a wide range of electrode potentials. These studies reveal that the rate of recovery increases as the potential becomes more negative, reaching a limiting rate below about  $-100$  mV.<sup>14</sup> The reactivation potentials used in each case were well below the switch potential for the particular enzyme: *Re* [NiFe]-MBH =  $+42$  mV; *Av* [NiFe]-hydrogenase =  $-126$  mV; *Dg* [NiFe]-hydrogenase =  $-158$  mV.

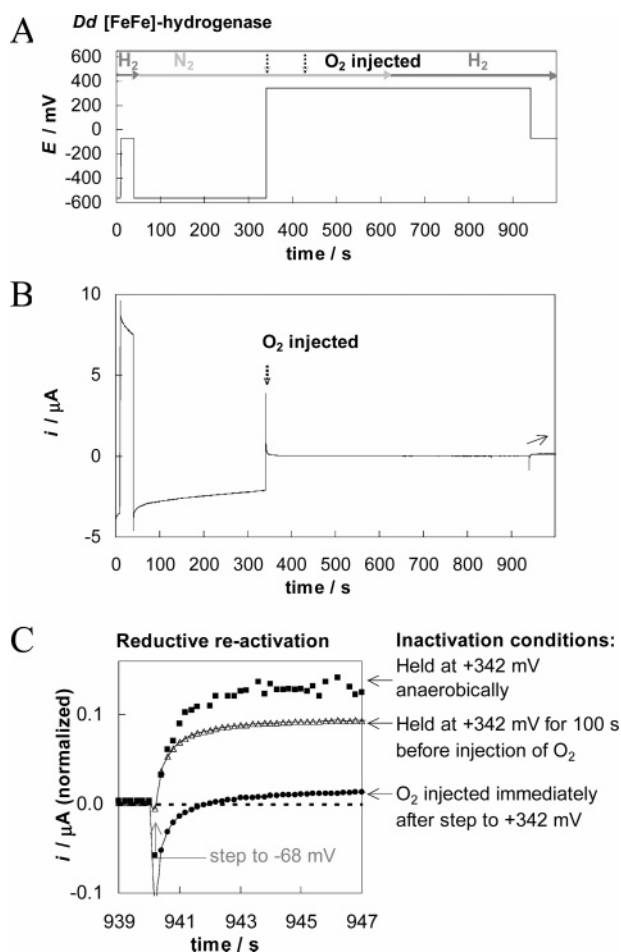
The typical potential step versus time sequence applied to the electrode for investigating the reactivation of the [NiFe]-hydrogenases is shown in Figure 7A, with the gas exchange steps marked. The resulting current response with time for the *Av* [NiFe]-hydrogenase is shown in Figure 7B. The electrode was initially polarized at  $-558$  mV with H<sub>2</sub> in the cell to ensure complete activation of the enzyme. A step to the designated reactivation potential then provides an indicator of initial enzyme electrocatalytic activity since the current recorded during this step is important for calculating the extent of recovery from an O<sub>2</sub> pulse, as discussed below. As in the preconditioning step, prior to the scans shown in Figure 6, the cell was then flushed with N<sub>2</sub> as the electrode was held at  $-558$  mV. The reduction current increases during this step, as H<sub>2</sub> inhibition of H<sup>+</sup> reduction is relieved. The potential was then stepped to  $+342$  mV and 200  $\mu$ L of O<sub>2</sub>-saturated buffer was injected immediately (to minimize high potential anaerobic inactivation) after the potential step. Upon injection of O<sub>2</sub>, the current drops to zero after the charging spike. The O<sub>2</sub> was then flushed out with N<sub>2</sub> (300 s) followed by H<sub>2</sub> (300 s), and the potential was stepped to the designated reactivation potential.

Figure 7C shows current versus time plots for the reductive reactivation stage of experiments conducted on the *Re*, *Av*, and *Dg* [NiFe]-hydrogenases as described above (and shown in Figure 7A). Differences in reactivation rates spanning several orders of magnitude are immediately obvious (these rates did not depend upon the coverage of the particular enzyme being addressed). Reactivation of *Re* [NiFe]-MBH is complete within seconds, whereas complete reactivation of the hydrogenases from the more anaerobic organisms, *A. vinosum* and *D. gigas*, requires 2 h or more. Figure 7D presents the corresponding plots of  $\ln(\text{current change})$  versus time. The data for the *Re* [NiFe]-MBH conform to a *single*, fast, first-order reactivation process with a rate constant  $k = 0.34 \pm 0.01 \text{ s}^{-1}$  ( $t_{1/2} = 2 \text{ s}$ ).<sup>55</sup> The rate constant is very similar to that measured under the same conditions when the enzyme has been inactivated *anaerobically*. For the *Av* and *Dg* [NiFe]-hydrogenases, *two* exponential phases are evident: a fast phase which is complete within seconds and a slow phase lasting hours. These phases have already been examined for the *Av* [NiFe]-hydrogenase in a detailed electrochemical study and correspond to reactivation of the Ready and Unready forms of the enzyme, respectively (Figure 2B).<sup>14</sup> Only the slow phases could be measured reliably. First-order rate constants for the *Av* and *Dg* hydrogenases are  $4.7 \pm 0.5 \times 10^{-4}$



**Figure 7.** Experiments designed to monitor the rate and extent of reductive reactivation of [NiFe]-hydrogenases after inactivation by O<sub>2</sub>. (A) Potential versus time trace showing the typical series of potential steps and gas exchanges employed. (B) Current versus time trace for the *A. vinosum* [NiFe]-hydrogenase. (C) Expanded current versus time traces for the reactivation stage for each enzyme at the potential indicated. (D) Plots of  $\ln(\text{current change})$  versus time for the reactivation stage. Current data for the *A. vinosum* and *D. gigas* hydrogenases were first adjusted for film loss (estimated from the current–time profile for an anaerobic potential step sequence). Conditions were: pH 6, 30 °C, 1 bar H<sub>2</sub>, electrode rotation at 2500 rpm, 2 mL initial cell solution volume prior to injection of 200  $\mu$ L of O<sub>2</sub>-saturated buffer.

(55) Kinetic measurements were carried out in triplicate, and error limits represent the standard deviation of the data set. Measurements were performed on samples of different coverage, and rates were found to be independent of coverage as expected. Here we examine the rate of change of catalytic turnover rate.



**Figure 8.** Experiments designed to investigate reductive reactivation of the *D. desulfuricans* [FeFe]-hydrogenase after anaerobic inactivation or inactivation by O<sub>2</sub> at different times. (A) Potential versus time trace showing the series of potential steps and gas exchanges employed. The two different O<sub>2</sub> injection points are indicated by dashed arrows. (B) Current versus time trace for an experiment in which O<sub>2</sub> is injected immediately after a step to +342 mV. (C) Current versus time traces showing reactivation stage at -68 mV after different inactivation protocols: ●, 200 μL of O<sub>2</sub>-saturated buffer injected immediately after the step to +342 mV; △, 200 μL of O<sub>2</sub>-saturated buffer injected 100 s after the potential step to +342 mV; ■, anaerobic inactivation at +342 mV. Currents have been normalized according to the level at 25 s (prior to exposure to O<sub>2</sub>). Other conditions were: pH 6, 30 °C, 1 bar H<sub>2</sub>, electrode rotation at 2500 rpm, 2 mL initial cell volume.

and  $3.3 \pm 0.7 \times 10^{-4} \text{ s}^{-1}$ , respectively, at pH 6 and 30 °C.<sup>55</sup> For comparison, the value for *Av* [NiFe]-hydrogenase obtained from electrochemical measurements reported by Lamle et al. at 45 °C is  $2.5 \pm 0.2 \times 10^{-3} \text{ s}^{-1}$ ,<sup>14</sup> while for the *Dg* enzyme, a value of  $4 \pm 1 \times 10^{-4} \text{ s}^{-1}$  has been reported by De Lacey et al. based on FTIR measurements at 40 °C.<sup>56</sup>

**The Extent of Reductive Reactivation after Inactivation by O<sub>2</sub>.** Finally, we consider the *extent* of recovery of the hydrogenases after exposure to a pulse of O<sub>2</sub>. In these experiments, as well as studies of other enzymes, we have consistently found that the act of stepping the potential contributes significantly to loss of electrocatalytic current, presumably due to destabilization of the noncovalently bound enzyme films (unpublished). The potential step/gas exchange sequence shown

in Figure 7A was therefore repeated under anaerobic conditions (with injection of anaerobic buffer) to allow us to take into account film loss (data not shown). The current level at the initial step to the reactivation potential (315 s, Figure 7B) functions as an indicator of initial enzyme activity and enables us to normalize the data for the anaerobic and aerobic step sequences against initial activity. Comparison of the final current in anaerobic and aerobic experiments (performed in triplicate) then provides an indication of the extent of activity irreversibly lost upon exposure of each enzyme to O<sub>2</sub>.

For *Re* [NiFe]-MBH, the final normalized current levels in anaerobic experiments are indistinguishable from those in aerobic experiments, showing that this enzyme suffers no permanent damage on exposure to O<sub>2</sub>. This is consistent with the position of *R. eutropha* at the top of the pond and the fact that the organism is a strict aerobe and must cope with O<sub>2</sub>. For the [NiFe]-hydrogenase from the semi-anaerobe, *A. vinosum*, electrochemical potential-step experiments have shown that less than 10% of the enzyme sample is subject to permanent damage following exposure to O<sub>2</sub>.<sup>14</sup> It was not possible to determine accurately the extent of O<sub>2</sub>-induced damage to the *Dg* [NiFe]-hydrogenase due to film loss over the course of the 4 h experiment.

Figure 8A shows similar experiments carried out on *Dd* [FeFe]-hydrogenase in which O<sub>2</sub> was added at high potential (+342 mV) under a H<sub>2</sub> atmosphere and then flushed out before a step to the reactivation potential (-68 mV, chosen on the basis of the reactivation potential in Figure 5). Figure 8B shows the current versus time trace for an experiment performed according to this protocol, and with O<sub>2</sub> injected immediately after the step to +342 mV. The reactivation step is expanded in Figure 8C (●), which reveals that very little activity is recovered. The experiment was also performed by holding the potential at +342 mV for 100 s to cause anaerobic inactivation *before* injecting O<sub>2</sub> (△). Significantly more activity is recovered in this case, but not as much as in an experiment performed under fully anaerobic conditions (■). These results support those shown in Figure 5C and discussed above, showing that exposure to O<sub>2</sub> of the *active* enzyme but not the *anaerobically* inactivated *Dd* [FeFe]-hydrogenase causes damage that may not be reversed by reduction.

Thus within this selection of enzymes, the extent of irreversible damage by O<sub>2</sub> increases significantly with decreasing O<sub>2</sub> tension experienced by the organisms from which these hydrogenases are isolated.

## Conclusions

The purpose of this paper has been to describe an effective and widely applicable way of measuring and placing on a *fully* quantitative scale the tolerance of isolated hydrogenases to O<sub>2</sub> and oxidizing environments. The following conclusions, summarized in Table 1, are empirical, but they define important questions to be addressed by more detailed structural investigations.

**1. Catalytic Bias: Capability for H<sub>2</sub> Oxidation versus H<sub>2</sub> Evolution.** All hydrogenases investigated catalyze H<sub>2</sub> oxidation, whereas under 1 bar H<sub>2</sub>, only the *Dd* [FeFe]-hydrogenase catalyzes the reverse reaction, H<sup>+</sup> reduction, to a significant extent. The *Re* [NiFe]-MBH is not only inactive for H<sup>+</sup>

(56) De Lacey, A. L.; Pardo, A. L. A.; Fernández, V. M.; Dementin, S.; Adryanczyk-Perrier, G.; Hatchikian, E. C.; Rousset, M. *J. Biol. Inorg. Chem.* **2004**, *9*, 636–642.

**Table 1.** Quantitative and Qualitative Comparisons among Hydrogenases Studied in This Investigation. All Data are for pH 6, 30 °C

enzyme, in order of position of organism in the pond	rate of anaerobic inactivation at pH 6	$E_{\text{switch}}$ at pH 6/ mV vs SHE <sup>a</sup> (following anaerobic inactivation)	rate of activation after anaerobic inactivation	reaction with O <sub>2</sub>	limiting rate constant for recovery from O <sub>2</sub> ( $t_{1/2}$ )	potential of onset of H <sub>2</sub> oxidation (reversible = "0") at 1 bar H <sub>2</sub> (mV)
<i>Ralstonia eutropha</i> [NiFe]-MBH	fast	+115	fast	fast, reversible	0.34 s <sup>-1</sup> (2 s)	>80
<i>Allochromatium vinosum</i> [NiFe]-hydrogenase	slow	-95	fast	fast, >90% reversible	4.7 × 10 <sup>-4</sup> s <sup>-1</sup> (25 min)	<30
<i>Desulfovibrio gigas</i> [NiFe]-hydrogenase	slow	-110	fast	fast, >70% reversible	3.3 × 10 <sup>-4</sup> s <sup>-1</sup> (35 min)	<30
<i>Desulfovibrio desulfuricans</i> [FeFe]-hydrogenase	fast	+75	fast	fast, irreversible	no recovery	0

<sup>a</sup> Errors are approximately ±10 mV.

reduction at 1 bar H<sub>2</sub>, but the potential for H<sub>2</sub> oxidation is shifted to markedly more positive potential by at least 80 mV (see point 3).

**2. Anaerobic Inactivation.** Under anaerobic conditions, the activity of all four hydrogenases switches off as the potential is raised and switches on again as the potential is swept or stepped to more negative values. Therefore, we believe that anaerobic oxidative inactivation is a fully reversible process; however, the switch potential ( $E_{\text{switch}}$ ) at which this occurs varies widely between the enzymes. The rates of inactivation also vary widely, being fast for the *Dd* and *Re* hydrogenases and slow for the *Av* and *Dg* enzymes at pH 6. For all the enzymes we have studied, it is true to say that the rate of reactivation is always equal to or higher than the rate of inactivation. For the *Av* and *Dg* [NiFe]-hydrogenases, the product of anaerobic inactivation is the well-characterized Ready state, also known as Ni-B or Ni<sub>r</sub>\*.<sup>13</sup> In the case of *Dd* [FeFe]-hydrogenase, the product is likely to be the Fe(II)Fe(II) state in which a water or hydroxide ligand is coordinated.<sup>57</sup>

**3. Redox-Potential Window for Activity.** The reversible inactivation at high potential defines the upper boundary of a "window of activity" for H<sub>2</sub> oxidation. The lower boundary is marked by the onset of H<sub>2</sub> oxidation, which is significantly shifted to more positive potential for *Re* [NiFe]-MBH compared to the other enzymes.

**4. Reactions with O<sub>2</sub>.** All four hydrogenases react with O<sub>2</sub> but to different extents of scale and reversibility. At one extreme, the *Dd* [FeFe]-hydrogenase reacts irreversibly with O<sub>2</sub> when O<sub>2</sub> is introduced to the active enzyme, but does not react with O<sub>2</sub> when it has been anaerobically inactivated; therefore, anaerobic oxidation protects the enzyme against O<sub>2</sub> damage as suggested previously.<sup>39-41</sup> For the other enzymes, reaction with O<sub>2</sub> is more reversible, and reactivation occurs at potentials close to  $E_{\text{switch}}$  measured in anaerobic studies. This is important because it defines the (thermodynamic) ease with which the O<sub>2</sub> challenge is overcome, thus the *Re* [NiFe]-MBH recovers even at a relatively high potential. For the *Av* and *Dg* [NiFe]-hydrogenases, the product depends on the reaction conditions, the Ready state being favored when plenty of reducing equivalents are present (under H<sub>2</sub> and at low potentials), whereas the Unready state (Ni-A or Ni<sub>u</sub>\*) is formed under electron-poor conditions.<sup>14</sup> The Unready state of these enzymes may contain a peroxide ligand in a bridging position between Ni and Fe atoms.<sup>24</sup> Reaction with *Re* [NiFe]-MBH is reversible and not

fully inhibited even at ambient levels of O<sub>2</sub>,<sup>4c</sup> however, the product(s) of the reactions, both anaerobic and under O<sub>2</sub>, have yet to be established. The rate of recovery (measured at a potential well below  $E_{\text{switch}}$ ) for the *Re* [NiFe]-MBH is by far the highest of the three [NiFe] enzymes. Our study now establishes the conditions required to generate well-defined states of *Re* [NiFe]-MBH for rigorous spectroscopic and structural investigations. On a wider note, the nature of irreversible inactivation of hydrogenases remains unclear. Oxygenation of residues, particularly cysteine, close to the fragile active sites is one option,<sup>24</sup> as is the loss of one or more diatomic ligands (CO, CN<sup>-</sup>) or damage to Fe-S clusters.

**5. Chemical and Biological Implications.** It is perhaps the very simplicity of the 2H<sup>+</sup>/H<sub>2</sub> interconversion that makes it so prone to interference by other small reactants such as O<sub>2</sub>. Indeed, O<sub>2</sub> also behaves as a substrate, in some cases causing permanent alteration of the active site. This is a central challenge for the development of biologically inspired synthetic catalysts.

The [NiFe]-MBH from the aerobe *R. eutropha* found in the O<sub>2</sub>-rich region at the top of the pond has adapted to maintain partial H<sub>2</sub> oxidation activity in the presence of O<sub>2</sub> and to undergo rapid and complete recovery of activity (with a half-life of ca. 2 s) at electrode potentials well above +100 mV following exposure to a pulse of O<sub>2</sub>. *Re* MBH is thus far more tolerant to O<sub>2</sub> than the *Av* and *Dg* enzymes both in kinetic and thermodynamic terms. Tolerance to O<sub>2</sub> may have evolved at the expense of catalytic reversibility since this enzyme begins to oxidize H<sub>2</sub> only at approximately 80 mV above the potential of the H<sup>+</sup>/H<sub>2</sub> couple and is a poor catalyst for H<sup>+</sup> reduction. The other organisms (*A. vinosum*, *D. gigas*, and *D. desulfuricans*) inhabit predominantly anaerobic environments, either in the sediment or anaerobic depths of waterways, and their hydrogenases are either inhibited or destroyed by O<sub>2</sub>. However, all three organisms may experience some O<sub>2</sub> under certain conditions,<sup>20</sup> and the [NiFe]-hydrogenases from *A. vinosum* and *D. gigas* are clearly equipped to recover activity after exposure to O<sub>2</sub>. The [FeFe]-hydrogenase from the anaerobe *D. desulfuricans* is an active catalyst both for H<sup>+</sup> reduction and H<sub>2</sub> oxidation within a narrow, anaerobic potential window, but activity switches off extremely rapidly and reversibly above 0 mV (pH 6). Generation of this anaerobically oxidized inactive state *in vivo* could protect against O<sub>2</sub> which causes essentially complete and irreversible damage to active forms of the enzyme.

Thus we demonstrate multiple modes of oxidative tolerance in hydrogenases in terms of (a) the kinetics of inactivation by O<sub>2</sub> or anaerobic oxidants; (b) the kinetics of reductive reactiva-

(57) Nicolet, Y.; Lemon, B. J.; Fontecilla-Camps, J. C.; Peters, J. W. *Trends Biochem. Sci.* **2000**, *25*, 138-143.

tion; (c) the potential dependence (thermodynamics) of reactivation; (d) the extent of recovery of activity after O<sub>2</sub> inactivation; and (e) the role of inactive states outside the catalytic cycle in protecting against O<sub>2</sub> damage. This strategy is likely to have widespread application because it provides a rich, quantitative picture using only a tiny amount of enzyme, thus paving the way for more detailed structural and spectroscopic investigations on specific states.

**Acknowledgment.** We thank the EPSRC and BBSRC (43/E16711) for supporting the research of F.A.A., K.A.V., and A.P. The work of O.L. and B.F. was supported by the DFG (Sfb498) and the Fonds der Chemischen Industrie. S.P.J.A. acknowledges

The Netherlands Organization for Scientific Research (NWO), Division for Chemical Sciences (CW), for financial support, and R.C. acknowledges the BBSRC and EU. We are grateful to E. C. Hatchikian for samples of *D. gigas* hydrogenase provided to R.C.

**Note Added in Proof.** A peroxide ligand located in a bridging position between the Ni and Fe atoms has recently been proposed for the Unready form of the [NiFe]-hydrogenase from *Desulfovibrio vulgaris* (Miyazaki F) (Ogata, H.; Hirota, S.; Nakahara, A.; Komori, H.; Shibata, N.; Kato, T.; Kano, K.; Higuchi, Y. *Structure* **2005**, *13*, 1635–1642.)

JA055160V